



Providing Choice & Value
Generic CT and MRI Contrast Agents

**FRESENIUS
KABI**

CONTACT REP

AJNR










Contribution of the MP2RAGE 7T Sequence in MS Lesions of the Cervical Spinal Cord

B. Testud, N. Fabiani, S. Demortière, S. Mchinda, N.L.
Medina, J. Pelletier, M. Guye, B. Audoin, J.P. Stellmann and
V. Callot

This information is current as
of July 28, 2025.

AJNR Am J Neuroradiol published online 10 August 2023
<http://www.ajnr.org/content/early/2023/08/10/ajnr.A7964>

Contribution of the MP2RAGE 7T Sequence in MS Lesions of the Cervical Spinal Cord

 B. Testud,  N. Fabiani,  S. Demortière,  S. Mchinda,  N.L. Medina,  J. Pelletier,  M. Guye,  B. Audoin,  J.P. Stellmann, and  V. Callot

ABSTRACT

BACKGROUND AND PURPOSE: The detection of spinal cord lesions in patients with MS is challenging. Recently, the 3D MP2RAGE sequence demonstrated its usefulness at 3T. Benefiting from the high spatial resolution provided by ultra-high-field MR imaging systems, we aimed to evaluate the contribution of the 3D MP2RAGE sequence acquired at 7T for the detection of MS lesions in the cervical spine.

MATERIALS AND METHODS: Seventeen patients with MS participated in this study. They were examined at both 3T and 7T. The MR imaging examination included a Magnetic Imaging in MS (MAGNIMS) protocol with an axial T2*-WI gradient recalled-echo sequence ("optimized MAGNIMS protocol") and a 0.9-mm isotropic 3D MP2RAGE sequence at 3T, as well as a 0.7-mm isotropic and 0.3-mm in-plane-resolution anisotropic 3D MP2RAGE sequences at 7T. Each data set was read by a consensus of radiologists, neurologists, and neuroscientists. The number of lesions and their topography, as well as the visibility of the lesions from one set to another, were carefully analyzed.

RESULTS: A total of 55 lesions were detected. The absolute number of visible lesions differed among the 4 sequences (linear mixed effect ANOVA, $P = .020$). The highest detection was observed for the two 7T sequences with 51 lesions each (92.7% of the total). The optimized 3T MAGNIMS protocol and the 3T MP2RAGE isotropic sequence detected 41 (74.5%) and 35 lesions (63.6%), respectively.

CONCLUSIONS: The 7T MP2RAGE sequences detected more lesions than the 3T sets. Isotropic and anisotropic acquisitions performed comparably. Ultra-high-resolution sequences obtained at 7T improve the identification and delineation of lesions of the cervical spinal cord in MS.

ABBREVIATIONS: GRE = gradient recalled-echo; LME = linear mixed effect; MAGNIMS = Magnetic Resonance Imaging in MS; UNI = uniform

MS is an immune-mediated disease that is responsible for the formation of demyelinating lesions of the CNS, in which spinal cord involvement is very common (80%–90%¹ of diagnosed patients) and responsible for a large portion of the

disability.^{2,3} Lesion assessment within the spinal cord, which is 1 of the 4 locations to confirm temporal and spatial dissemination,⁴ is thus crucial for the diagnosis of MS and for eliminating various differential diagnoses.

The Magnetic Resonance Imaging in MS (MAGNIMS) guidelines⁵ recommend the study of the entire spinal cord using at least 2 MR images (eg, sagittal T2WI, proton density-weighted or STIR sequences, and/or T1WI postgadolinium) to increase the confidence in lesion detection. Axial T2WI or T2*-WI sequences are also proposed to corroborate, characterize, or confirm the presence of visible lesions. Indeed, previous studies demonstrated their relevant value for both improved lesion detection and confidence in the interpretation.^{6–8}

In practice, lesion detection in the spinal cord of patients with MS is difficult and challenging, even using 3T MR images. These difficulties are related to physiological noise such as breathing or CSF flow⁹ and to the relatively low spatial resolution of sequences acquired at lower field strengths such as 1.5 and 3T, resulting in

Received April 17, 2023; accepted after revision July 6.

From the Center for Magnetic Resonance in Biology and Medicine (B.T., N.F., S.D., S.M., N.L.M., J.P., M.G., B.A., J.P.S., V.C.), Aix-Marseille University, Centre national de la recherche scientifique, Marseille, France; Assistance Publique-Hopitaux de Marseille (B.T., N.F., S.D., S.M., N.L.M., J.P., M.G., B.A., J.P.S., V.C.), Hôpital Universitaire Timone, CEMEREM, Marseille, France; and Department of Neurology (S.D., J.P., B.A.), Assistance Publique-Hopitaux de Marseille, Hôpital Universitaire Timone, Marseille, France.

This work was supported by the Fondation pour l'Aide à la recherche sur la Sclérose en Plaques and the Centre National de la Recherche Scientifique. It was performed within a laboratory member of the France Life Imaging network (grant ANR-11-INBS-0006), on the platform 7T-AMI, a French "investissements d'avenir" program (grant ANR-11-EQPX-0001).

Please address correspondence to Benoit Testud, MD, Centre d'exploration métabolique par résonance magnétique, APHM La Timone, 264 Saint-Pierre St, 13385 Marseille cedex, France; e-mail: Benoit.testud@ap-hm.fr

<http://dx.doi.org/10.3174/ajnr.A7964>

Table 1: Main sequence parameters

Magnetic Field Sequence	3T				7T	
	T2*-WI	T2WI	STIR-WI	MP2RAGE	MP2RAGE Isotropic	MP2RAGE Anisotropic
Dimension/orientation	2D Axial	2D Sagittal	2D Sagittal	3D Sagittal	3D Coronal	3D Axial
TR (sec)	0.5	4	3.2	4	5	5
TE (ms)	27	113	53	2.48	2.15	3.05
FOV (mm)	180	280	320	300	260	256
Resolution (mm ³)	0.5 × 0.5 × 5	1.1 × 0.9 × 2	0.9 × 0.7 × 3	0.9 × 0.9 × 0.9	0.7 × 0.7 × 0.7	0.3 × 0.3 × 4
Slices	9 Per slab, 2 Slabs ^a			176	192	64 Slices per slab, 1 or 2 Slabs ^{a,b}
Acq. time (min)	5.26	1.54	2.18	7.18	8.47	6.02/Slab

Note:—Acq. indicates acquisition.

^aPlaced perpendicular to the cord.

^bDepending on cord curvature.

partial volume effects. Due to the increase in both SNR and the contrast-to-noise ratio, ultra-high-field MR imaging at 7T of the cervical spinal cord now allows a higher spatial resolution and more defined anatomic details,^{10,11} which can help detect and delineate cervical spinal MS lesions compared with the 3T evaluation.^{11,12} 7T also reveals information about lesion distribution in the spinal cord.¹³ In the meantime, Demortière et al¹⁴ illustrated the value of the 3D MP2RAGE¹⁵ sequence at 3T, which allowed the detection of a greater number of MS lesions than sequences recommended by the MAGNIMS consensus. The MP2RAGE sequence has been used broadly in the brain^{16,17} and was more recently optimized for the cervical spinal cord at both 3T and 7T.^{18,19}

In line with these results, our goal was to determine the potential added value of the 7T 3D MP2RAGE sequence over a 3T MR imaging evaluation for detecting cervical spinal cord lesions in patients with MS.

MATERIALS AND METHODS

Population

We analyzed data collected from a prospective study focusing on the 3T and 7T multimodal assessment of the spinal cord in MS that took place from December 2017 to September 2019. The study was approved by the local Aix-Marseille University ethics committee, and written informed consent was collected from each participant before the MR imaging examinations. Inclusion criteria were a diagnosis of MS according to the revised McDonald 2017 criteria,⁴ patients older than 18 years of age, clinical symptoms suggesting spinal cord involvement, and an MR imaging examination performed at least 3 months after steroid infusion. Patients with uncertain diagnosis, in relapse, or with a standard contraindication to an MR imaging examination such as incompatible implanted equipment, claustrophobia, agitation, and intrabody metal fragments were excluded.

Image Acquisition

All MR imaging examinations were performed on the same day using 3T (Verio; Siemens) and 7T (Magnetom; Siemens) MR imaging systems. MR imaging at 3T was performed using the body coil for transmission and standard 12-channel head, 4-channel neck, and 24-channel spine matrix array coils for reception. MR imaging at 7T was performed using a customized 8Tx/8Rx

transceiver coil array (RAPID Biomedical), used in the compact polarimetric mode. The 7T examination was performed in the morning, and the 3T examination, in the afternoon. The 3T MR imaging protocol included the sequences recommended by the MAGNIMS consensus,²⁰ ie, sagittal 2D T2 TSE-WI and STIR-WI, as well as an axial 2D T2*-WI multiecho gradient recalled-echo (GRE) sequence, hence forming an “optimized MAGNIMS” set. The 3T protocol also included 1 sagittal 3D MP2RAGE sequence with isotropic resolution (0.9 mm³), which covered both the brain and cervical spinal cord¹⁸ and provided 2 contrasted images (TI1, TI2) from which a uniform (UNI) image and a T1 map were derived.

At 7T, the MR imaging protocol included an axial 3D MP2RAGE sequence with a spatial resolution of 0.3 × 0.3 × 4 mm³ and a coronal 3D MP2RAGE sequence with an isotropic spatial resolution of 0.7 mm³. A fast T2 TSE sequence was also performed to locate the vertebral level on the 3D MP2RAGE anisotropic sequence.

The main sequence parameters are summarized in Table 1.

Lesion Detection and Scoring

Lesion detection was performed by a consensus of a senior neuro-radiologist (B.T.), a senior neurologist (S.D.), a neuroradiology resident (N.F.), and 3 neuroscientists specialized in spinal cord MR imaging and MS (S.M., N.L.M., and V.C.), all blinded to clinical data, using the Horos Viewer (<https://horosproject.org>).

Each set (Optimized MAGNIMS, 3T MP2RAGE, 7T MP2RAGE with isotropic resolution, and 7T MP2RAGE with anisotropic resolution) was viewed successively and individually by the reading group with a 3-week delay between each session, and the viewing order of the subjects was randomly generated for each set to avoid memory bias. The 3T sequences were observed before the 7T sequences to avoid potential learning biases on 3T images due to more informative 7T images. Finally, once all imaging sets had been observed, the 4 imaging sets were displayed simultaneously to obtain a lesion concordance among imaging sets. The UNI image or the T1 map of the 3D MP2RAGE sequences or both were used for interpretation. Lesions visible on at least 2 consecutive slices and whose radiologic characteristics were in favor of MS lesions were retained for the lesion count. For each lesion, the vertebral level (from C1 to C7), the location in the transverse section plane (anterior,

lateral, posterior), and the involvement of the white and/or gray matter were recorded. Lesions in front of the intervertebral disc were considered to belong to the overlying level.

Statistics

We performed descriptive statistics on the cohort and compared the total number of lesions visualized per sequence. We compared the absolute number of visible lesions over all sequences by computing the ANOVA of a linear mixed effect (LME) model, accounting for recurrent measurements in patients. We also computed the Dice score for pair-wise comparisons as an indicator of

the similarity. The LME approach was also applied to explore differences among spinal cord levels. *P* values below .05 were considered significant. All statistical analyses were performed using R statistical and computing software (<http://www.r-project.org>).

RESULTS

Population

Of the 19 patients, 2 were excluded because the spinal cord presented with inseparable lesions (diffuse aspect). Consequently, 17 patients participated in the study (12 women/5 men; mean age, 30.2 [SD, 9.9] years; range, 20–41 years), all with a relapsing-remitting form of the disease. The study population presented with a mild disability, with a median Expanded Disability Status Scale score of 1.5 (mean, 0.9 [SD, 1]; range, 0–3) and a short disease duration, with a median of 17 months (mean, 40.8 [SD, 7.3] months; range, 6–189 months). Six patients in the study had no therapy. Detailed demographic data, clinical characteristics, and lesion counts, reported as the maximum number of lesions visualized in each patient, are summarized in Table 2. The 7T isotropic resolution 3D MP2RAGE sequence was missing for 3/17 patients.

Lesion Characteristics

Four patients presented with no lesions. Among the 14 patients who had 4 complete sets of images, 55 lesions were identified in total, 31 located in the posterior part of the spinal cord (56.4%), 17 lateral (30.9%), 6 anterior (10.9%), and 1 central. Twenty-eight lesions (50.9%) affected the white matter only; the remaining affected both the white and gray matter. Figure 1 shows the proportion of lesions detected by each sequence on the spinal cord globally and for each level, considering only the patients who had all 4 imaging sets. The absolute number of visible lesions differed among the 4 sequences (LME ANOVA, *P* = .020). The highest

Table 2: Demographic and clinical characteristics

Patients	Age (yr)	Sex	Disease Course	Disease Duration (mo)	EDSS	Lesion Count
P1	40	M	RR	95	2	7
P2 ^a	20	F	RR	58	2.5	3
P3	30	F	RR	87	1.5	6
P4	27	F	RR	17	3	6
P5	23	F	RR	47	0	5
P6	31	F	RR	6	0	0
P7	35	F	RR	33	1	3
P8	28	F	RR	6	0	3
P9	38	F	RR	7	1	0
P10	33	M	RR	17	0	3
P11	31	F	RR	189	0	12
P12	41	F	RR	45	1	7
P13	26	M	RR	12	0	3
P14	20	M	RR	44	0	0
P15	30	F	RR	10	1	0
P16 ^a	35	M	RR	11	2	12
P17 ^a	26	F	RR	10	1	8

Note:—RR indicates relapsing-remitting; F, female; M, male; EDSS, Expanded Disability Status Scale.

^a The patients who could not have the examination with the 7T isotropic MP2RAGE sequence.

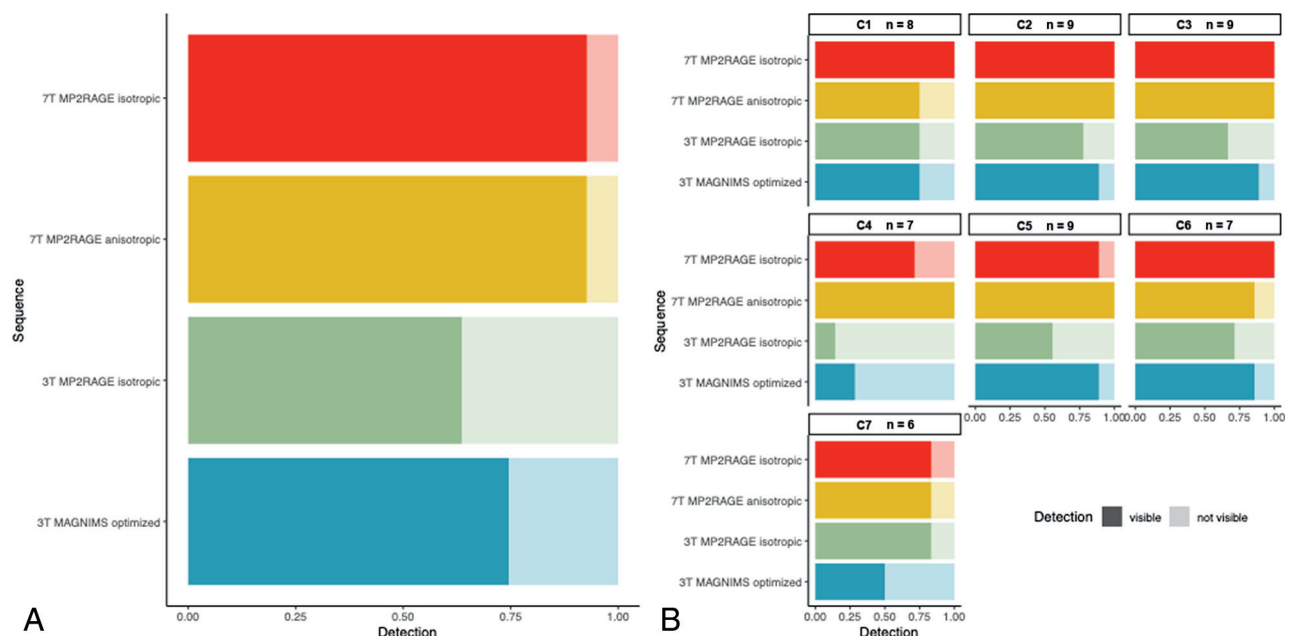


FIG 1. Proportion of lesion detection by sequence (A) and by sequence per vertebral level (B) for the patients having the 4 imaging sets (14 patients). The number of lesions (*n*) is detected for each cervical level.

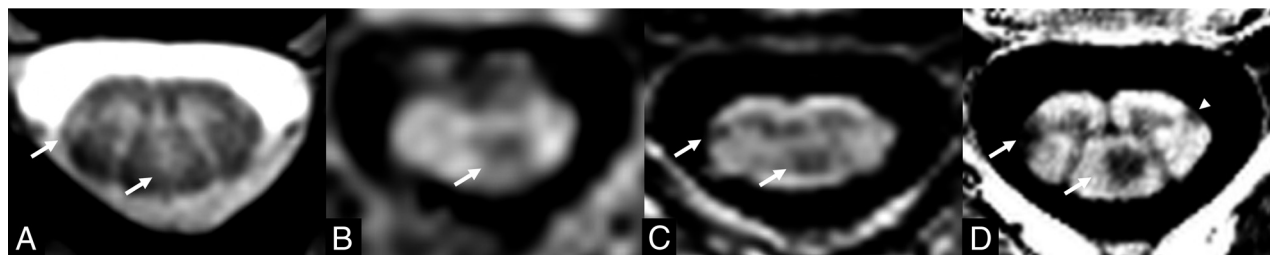


FIG 2. Axial presentation at the C4 level for patient P11. Images were acquired with the T2*-WI GRE (A), 3T UNI MP2RAGE (B), 7T isotropic UNI MP2RAGE (C), and 7T anisotropic UNI MP2RAGE (D) sequences. The posterior lesion was visible on each image, the right lateral lesion was not visible on the 3T UNI MP2RAGE sequence (B), and the left lateral lesion (white arrowhead) was only detected with the 7T anisotropic UNI MP2RAGE sequence (D).

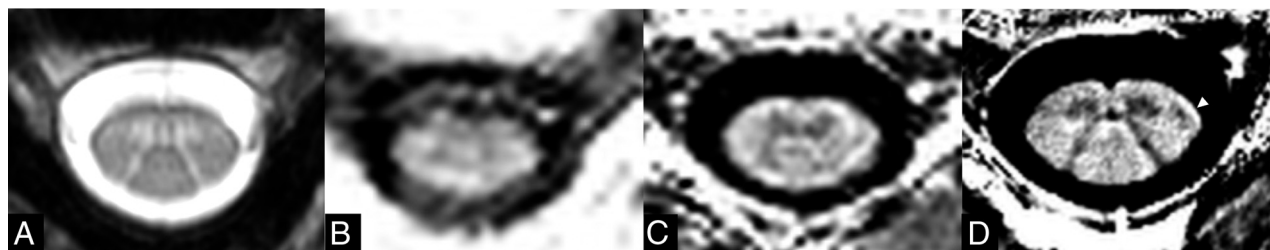


FIG 3. A patient P13 presenting with a C4 left lateral lesion (arrowhead). The lesion was not detected on axial T2*-WI GRE image (A), the 3T UNI MP2RAGE (B), nor the 7T isotropic UNI MP2RAGE (C). It was only detected using the 7T anisotropic UNI MP2RAGE (D).

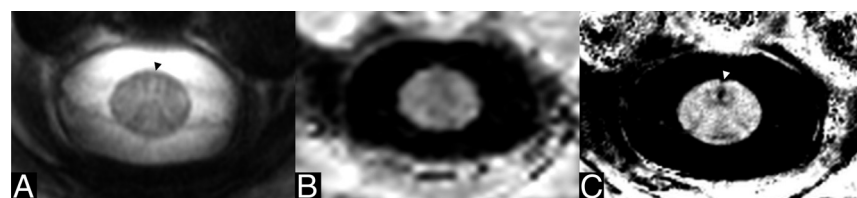


FIG 4. Patient P17 presented with a small lesion (arrowhead) in contact with the anterior fissure of the spinal cord at the C1–C2 level. The lesion was seen on a T2*-WI GRE (A) image, not seen on 3T UNI MP2RAGE (B), and easily seen on 7T anisotropic UNI MP2RAGE (C) image.

that was too low: Three lesions were not detected on the 7T MP2RAGE isotropic sequence but were visible on the 7T MP2RAGE anisotropic sequence and 2 lesions that had a very small diameter in the sagittal and coronal planes were not seen on the 7T MP2RAGE anisotropic sequence due to section thickness partial volume effects but were visible on the 7T MP2RAGE isotropic sequence.

detection was observed for the two 7T sequences with 51 lesions each (LME ANOVA, $P = 1$, Dice = 0.92). Detection at 7T was higher on average (the whole cervical cord considered) than at 3T (LME ANOVA 3T versus 7T, $P = .003$, Dice = 0.59). Figures 2–5 show examples of lesions that were only visible at 7T. For the 3T MP2RAGE isotropic sequence, 35 lesions were detected (Dice = 0.57), which were not significantly less than the optimized MAGNIMS protocol with 41 lesions (Dice = 0.61; LME ANOVA, $P = .239$). The spatial distribution of lesions showed the highest absolute numbers at the C2, C3, and C5 levels.

Concerning patients who could not have the examination with the 7T isotropic MP2RAGE sequence, the highest lesion detection was with the 7T anisotropic sequence with 23 lesions. 3T MP2RAGE and optimized MAGNIMS performed similarly with 15 lesions detected each.

Among all patients in the cohort, 8/78 lesions (10%) were not detected at 7T, 4 with the 7T MP2RAGE anisotropic and 4 with the 7T MP2RAGE isotropic sequences. For 3 lesions, this issue was related to artifacts that interfered with the lesion detection. For the 5 remaining lesions, this was related to having a spatial resolution

DISCUSSION

This study showed promising results on the contribution of ultra-high-field (7T) 3D MP2RAGE sequences to cervical spinal cord involvement in MS. In addition, it provides several useful comments for clinical research practice.

In line with the literature,¹¹ the expected increase in the contrast-to-noise ratio and SNR at ultra-high field¹⁰ and the high resolution allowed detection of a greater number of lesions than at 3T. The study additionally provides an objective 3T/7T comparison using the MP2RAGE sequence, compared with Dula et al,¹¹ who compared slightly different contrasts (7T T2*-WI fast-field echo versus 3T T2WI FSE axial sequences). The readers experienced an improved viewing even in the case of numerous and coalescing lesions at 7T compared with 3T. 7T 3D-MP2RAGE allows better lesion delineation, leading to a more accurate and reliable counting compared with 3T imaging sets. The readers were able, on several occasions, to easily confirm the presence of hardly visible lesions or lesions referred to as nonspecific signal anomalies on 3T images, even an inexperienced reader. Among the patients who had the two 7T MP2RAGE sequences, we did

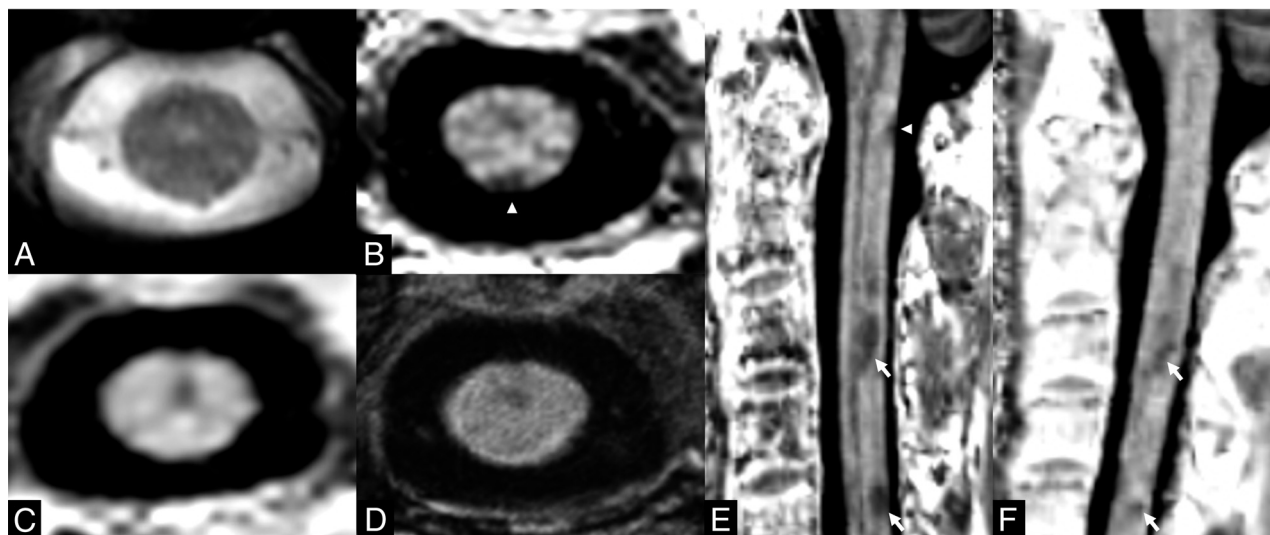


FIG 5. Patient P3 presented with a small posterior lesion (white arrowhead) at the C1 level that was not seen on axial T2*-WI GRE (A) image nor with 3T UNI MP2RAGE (B). At 7T, the lesion was seen on the axial plane of the isotropic UNI MP2RAGE sequence (C), but it was not seen on the anisotropic 7T UNI MP2RAGE image (D). The sagittal plane (E) of the 7T isotropic UNI MP2RAGE sequence shows that this lesion (white arrowhead) has a small height. This lesion is not seen on the sagittal 3T UNI MP2RAGE (F). Additional lesions (white arrows) can be seen at the C3 and C5 levels on both sagittal planes (E and F).

not observe any difference in terms of detection. All visible lesions at 3T were identified on 1 of the two 7T sets, and only 8 lesions visible at 3T were not seen on 1 of the two 7T sets in the entire cohort. Not detecting lesions at 7T was due to artifacts or very small lesions in the z-axis (respect to transverse) plane, which penalized the 7T MP2RAGE anisotropic (respect to 7T MP2RAGE isotropic) sequence. The 7T 3D MP2RAGE sequence with isotropic resolution, which had a long acquisition time, was acquired last in our protocol, potentially making it more vulnerable to motion artifacts.

Considering the 3T data sets, Demortière et al¹⁴ previously reported improved lesion detection using the 3T MP2RAGE sequence compared with the conventional MAGNIMS set. In our protocol, an “optimized” MAGNIMS set including an axial 2D T2*-WI GRE sequence, providing high in-plane axial resolution (0.5 mm) with high white matter/gray matter/lesion contrast, was used instead. Despite being considered as optional according to the latest guidelines,⁵ the T2*-WI GRE sequence, nonetheless, allowed the detection of many lesions not visible otherwise, thus explaining the relative success of our optimized MAGNIMS compared with the 3T MP2RAGE. The relatively poor performance of 3T sequences at the C4 level may be attributed to the acquisition of the T2*-WI sequence in 2 slabs, where C4 constitutes the junction between the slabs. This acquisition may have interfered with the viewing. No specific reason was identified for the 3T MP2RAGE sequence, and this issue should be further investigated in a larger cohort. An objective comparison among 2D T2*-WI GRE, MP2RAGE, and the conventional MAGNIMS set at 3T was beyond the scope of the present study. However, such a comparison may be of interest in the future because the 3D MP2RAGE sequence offers a shorter acquisition time than the optimized MAGNIMS, as well as simultaneous coverage of both the brain and cervical cord¹⁸ with an isotropic resolution. It would thus be particularly relevant for MS and

may be a good alternative to the MAGNIMS set in clinical practice.

Regarding the lesion location, lesions were more frequent in the upper cervical cord (C2–C3), and lesions in the posterior and lateral cords were the most numerous, in agreement with the literature.^{21,22}

No specific radiologic pattern was better detected at 7T than at 3T. However, the gain in contrast and resolution allowed the detection of small lesions in locations that were not easily accessible at 3T, such as the anterior cord or on the outer edge of the cord in contact with the CSF. In addition, readers experienced a learning effect of imaging at 7T, ie, some lesions not reported at 3T could subsequently be retained after the 7T reading. Lefeuvre et al²³ could establish the existence of subpial white matter lesions using an animal experimental autoimmune encephalomyelitis model of the spinal cord, which has not been reported so far in the human spinal cord. These lesions were revealed by ex vivo ultra-high-resolution 7T MR imaging (3D T2*-WI with an in-plane resolution of 70 μ m and a section thickness of 200 μ m) and, thus, were unrevealed by our study.

In this study, we chose to focus on the MP2RAGE sequence, which was shown to be more robust. While the T2*-WI of the spinal cord at 7T is a high-reward sequence with high resolution and a high contrast for lesion detection,^{11,13,23} it is also a high-risk sequence, which is sensitive to inhomogeneities of the magnetic field and to motion artifacts.²⁴

Our study has several limitations. It is a retrospective study with a small sample size. Although our lesion features are comparable with those in the literature and provide a representative sample of spinal cord injury in MS, a further study with a larger sample size is needed to confirm our results.

The learning effect on readers may also be a potential bias in this work, which may have led to an improvement in the performance of the readers. Nonetheless, we assume that this was

minimized by interpreting the images in different sessions with a minimum interval of 3 weeks and presenting the patients in a random order.

For each patient, the 7T MR imaging examination was performed first, and this choice may have benefited the 7T evaluation by having less risk of motion artifacts than the 3T evaluation performed later. However, patients had a long break between the 2 examinations, which limited this bias. Last, our reading process did not allow reporting of individual confidence, nor did we perform a concordance among readers, possibly limiting the relevance of our results. Nevertheless, it allowed establishing a level-by-level lesion concordance among imaging sets.

From a practical point of view, 7T sequences detected more lesions than 3T sequences. However, this added value in lesion detection must be balanced with a potentially longer acquisition time. While the 3T MP2RAGE sequence seems to be an interesting alternative to the MAGNIMS set with a T2* axial sequence, given the equivalent acquisition time, similar lesion detection, and the possibility of covering the brain (included in the FOV), the 7T sequences are more oriented toward more precise indications. For example, the use of the 7T MP2RAGE sequence with ultra-high resolution in the axial plane could contribute beyond MS in the fine characterization of cervical myelitis or to better appreciate possible doubtful lesions.

CONCLUSIONS

Due to increased spatial resolution, 7T 3D MP2RAGE sequences allowed improved identification and delineation of lesions compared with 3T. It would be interesting to study longitudinally the potential impact of the 7T MP2RAGE sequences on the management of patients with MS. The clinical research perspectives of 7T MR imaging now require technical advances to image the thoracic and lumbar spinal cord and to reduce the acquisition time in implementing a “compressed-sensing” version of the method²⁵ for the cord. While we are waiting for the full development and greater availability of 7T systems, it would also be interesting to investigate further the potential of the 3T 3D MP2RAGE protocol dedicated to both the brain and cervical spinal cord as an alternative to the conventional MAGNIMS protocol.

ACKNOWLEDGMENTS

The authors thank V. Gimenez, L. Pini, C. Costes, P. Durozard, A. Rico, A. Maarouf, and M.P. Ranjeva for study logistics, as well as Tobias Kober from Siemens for MR image support.

Disclosure forms provided by the authors are available with the full text and PDF of this article at www.ajnr.org.

REFERENCES

- Bot JC, Blezer EA, Kamphorst W, et al. **The spinal cord in multiple sclerosis: relationship of high-spatial-resolution quantitative MR imaging findings to histopathologic results.** *Radiology* 2004;233:531–40 [CrossRef Medline](#)
- Gass A, Rocca MA, Agosta F, et al; MAGNIMS Study Group. **MR monitoring of pathological changes in the spinal cord in patients with multiple sclerosis.** *Lancet Neurol* 2015;14:443–54 [CrossRef Medline](#)
- Brownlee WJ, Altmann DR, Prados F, et al. **Early imaging predictors of long-term outcomes in relapse-onset multiple sclerosis.** *Brain* 2019;142:2276–87 [CrossRef Medline](#)
- Thompson AJ, Banwell BL, Barkhof F, et al. **Diagnosis of multiple sclerosis: 2017 revisions of the McDonald criteria.** *Lancet Neurol* 2018;17:162–73 [CrossRef Medline](#)
- Wattjes MP, Ciccarelli O, Reich DS, et al; North American Imaging in Multiple Sclerosis Cooperative MRI guidelines working group. **2021 MAGNIMS–CMSC–NAIMS consensus recommendations on the use of MRI in patients with multiple sclerosis.** *Lancet Neurol* 2021;20:653–70 [CrossRef Medline](#)
- Weier K, Mazraeh J, Naegelin Y, et al. **Biplanar MRI for the assessment of the spinal cord in multiple sclerosis.** *Mult Scler* 2012;18:1560–69 [CrossRef Medline](#)
- Galler S, Stellmann JP, Young KL, et al. **Improved lesion detection by using axial T2-weighted MRI with full spinal cord coverage in multiple sclerosis.** *AJNR Am J Neuroradiol* 2016;37:963–69 [CrossRef Medline](#)
- Bergers E, Bot JC, De Groot CJ, et al. **Axonal damage in the spinal cord of MS patients occurs largely independent of T2 MRI lesions.** *Neurology* 2002;59:1766–71 [CrossRef Medline](#)
- Stroman PW, Wheeler-Kingshott C, Bacon M, et al. **The current state-of-the-art of spinal cord imaging: methods.** *Neuroimage* 2014;84:1070–81 [CrossRef Medline](#)
- Barry RL, Vannesjo SJ, By S, et al. **Spinal cord MRI at 7T.** *Neuroimage* 2018;168:437–51 [CrossRef Medline](#)
- Dula AN, Pawate S, Dortch RD, et al. **Magnetic resonance imaging of the cervical spinal cord in multiple sclerosis at 7T.** *Mult Scler* 2016;22:320–28 [CrossRef Medline](#)
- Kreiter DJ, van den Hurk J, Wiggins CJ, et al. **Ultra-high field spinal cord MRI in multiple sclerosis: where are we standing? A literature review.** *Mult Scler Relat Disord* 2022;57:103436 [CrossRef Medline](#)
- Ouellette R, Treaba CA, Granberg T, et al. **7 T imaging reveals a gradient in spinal cord lesion distribution in multiple sclerosis.** *Brain* 2020;143:2973–87 [CrossRef Medline](#)
- Demortière S, Lehmann P, Pelletier J, et al. **Improved cervical cord lesion detection with 3D-MP2RAGE sequence in patients with multiple sclerosis.** *AJNR Am J Neuroradiol* 2020;41:1131–34 [CrossRef Medline](#)
- Marques JP, Kober T, Krueger G, et al. **MP2RAGE, a self bias-field corrected sequence for improved segmentation and** *Neuroimage* 2010;49:1271–81 [CrossRef Medline](#)
- Okubo G, Okada T, Yamamoto A, et al. **MP2RAGE for deep gray matter measurement of the brain: a comparative study with MP2RAGE—MP2RAGE for deep gray matter measurement.** *J Magn Reson Imaging* 2016;43:55–62 [CrossRef Medline](#)
- Marques JP, Gruetter R. **New developments and applications of the MP2RAGE sequence: focusing the contrast and high spatial resolution R1 mapping.** *PLoS One* 2013;8:e69294 [CrossRef Medline](#)
- Forodighasemabadi A, Rasoanandrianina H, El Mendili MM, et al. **An optimized MP2RAGE sequence for studying both brain and cervical spinal cord in a single acquisition at 3T.** *Magn Reson Imaging* 2021;84:18–26 [CrossRef Medline](#)
- Massire A, Taso M, Besson P, et al. **High-resolution multi-parametric quantitative magnetic resonance imaging of the human cervical spinal cord at 7T.** *Neuroimage* 2016;143:58–69 [CrossRef Medline](#)
- Filippi M, Rocca MA, Ciccarelli O, et al; MAGNIMS Study Group. **MRI criteria for the diagnosis of multiple sclerosis: MAGNIMS consensus guidelines.** *Lancet Neurol* 2016;15:292–303 [CrossRef Medline](#)
- Eden D, Gros C, Badji A, et al. **Spatial distribution of multiple sclerosis lesions in the cervical spinal cord.** *Brain* 2019;142:633–46 [CrossRef Medline](#)
- Kearney H, Miller DH, Ciccarelli O. **Spinal cord MRI in multiple sclerosis: diagnostic, prognostic and clinical value.** *Nat Rev Neurol* 2015;11:327–38 [CrossRef Medline](#)

23. Lefeuvre JA, Guy JR, Luciano NJ, et al. **The spectrum of spinal cord lesions in a primate model of multiple sclerosis.** *Mult Scler* 2020;26:284–93 [CrossRef](#) [Medline](#)
24. Frebourg G, Massire A, Pini L, et al. **The good, the bad and the ugly: a retrospective study of human cervical spinal cord image quality at 7T.** In: *Proceedings of the Annual Meeting and Exhibition of the International Society for Magnetic Resonance in Medicine*, May 15–20, 2021; Virtual
25. Mussard E, Hilbert T, Forman C, et al. **Accelerated MP2RAGE imaging using Cartesian phyllotaxis readout and compressed sensing reconstruction.** *Magn Reson Med* 2020;84:1881–94 [CrossRef](#) [Medline](#)